Effect of Double Dispersion on Mixed Convection Heat and Mass Transfer in Non-Darcy Porous Medium

P. V. S. N. Murthy[1]
Department of Mathematics,
I.I.T.–Madras,
Madras 600 036, India

Similarity solution for the problem of hydrodynamic dispersion in mixed convection heat and mass transfer from vertical surface embedded in porous media has been presented. The flow induced by the density variations is comparable with the freestream flow. The heat and mass transfer in the boundary layer region for aiding and opposing buoyancies in both aiding and opposing flows has been analyzed. The structure of the flow, temperature, and concentration fields in the Darcy and non-Darcy porous media are governed by complex interactions among the diffusion rate (Le) and buoyancy ratio (N) in addition to the flow driving parameter (Ra/Pe). The flow, temperature, and concentration fields are analyzed and the variation of heat and mass transfer coefficients with the governing parameters are presented. [S0022-1481(00)00703-9]

Keywords: Boundary Layer, Dispersion, Heat Transfer, Mass Transfer, Mixed Convection, Porous Media

1 Introduction

Thermal and solutal transport by fluid flowing through a porous matrix is a phenomenon of great interest from both the theory and application point of view. Heat transfer in the case of homogeneous fluid-saturated porous media has been studied with relation to different applications like dynamics of hot underground springs, terrestrial heat flow through aquifer, hot fluid and ignition front displacements in reservoir engineering, heat exchange between soil and atmosphere, flow of moisture through porous industrial materials, and heat exchanges with fluidized beds. Mass transfer in isothermal conditions has been studied with applications to problems of mixing of fresh and salt water in aquifers, miscible displacements in oil reservoirs, spreading of solutes in fluidized beds and crystal washers, salt leaching in soils, etc. Prevention of salt dissolution into the lake waters near the sea shores has become a serious problem of research.

Coupled heat and mass transfer phenomenon in porous media is gaining attention due to its interesting applications. The flow phenomenon is relatively complex rather than that of the pure thermal convection process. Processes involving heat and mass transfer in porous media are often encountered in the chemical industry, in reservoir engineering in connection with thermal recovery process, and in the study of dynamics of hot and salty springs of a sea. Underground spreading of chemical wastes and other pollutants, grain storage, evaporation cooling, and solidification are the few other application areas where the combined thermo-solutal natural convection in porous media are observed. Combined heat and mass transfer by free convection under boundary layer approximations has been studied by Bejan and Khair [1], Lai and Kulacki [2], and Murthy and Singh [3]. Coupled heat and mass transfer by mixed convection in Darcian fluid-saturated porous medium has been analyzed by Lai [4]. The free convection heat and mass transfer in a porous enclosure has been studied recently by Angirasa et al. [5].

The porous medium inertial effects have been proved to be important for moderate and fast flows, i.e., when the pore diameter-dependent Reynolds number is greater than the order of unity. For low-porosity media, the Forchheimer flow model has been proved to be appropriate and it has been widely used in the works of Vafai and Tien [6,7], Whitaker [8], etc. When the inertial effects are prevalent, the thermal and solutal dispersion effects become important, and these effects are very significant in forced and mixed convection flows and in vigorous natural convection flows as well. Thermal dispersion effects have been studied at length by researchers such as Bear [9], Kvernvold and Tyvand [10], Plumb [11], Hong and Tien [12], Hong et al. [13], Cheng and Vortmeyer [14], Lai and Kulacki [15], Amiri and Vafai [16], Gorla et al. [17], and Murthy and Singh [18,19]. A brief review on thermal dispersion can be found in Bear [9] and Nield and Bejan [20]. Kvernvold and Tyvand [10] argued that better agreement between the theoretical prediction and experimental data can be obtained when thermal dispersion effects are taken into consideration appropriately.

Coupled heat and mass transfer phenomenon in non-Darcy flows are studied by Karimi-Fard et al. [21] and Murthy and Singh [3]. The complexity of the flow increases when higher order effects like thermal and solutal dispersion, wall channeling, and porosity variations are considered in the medium. A numerical study of double-diffusive free-convection heat and mass transfer in a square cavity filled with a porous medium has been done by Karimi-Fard et al. [21]. A more general flow equation (Darcy-Forchheimer-Brinkman), coupled with energy and concentration equations, are solved using a finite volume technique. The investigation showed that the inertial and boundary effects have a profound effect on the double-diffusive convection. The study is valid for $N=1$ and it neglected the effect of double dispersion which is most important in the non-Darcy mixed convection. A similarity solution has been presented in Murthy and Singh [3] for the free-convection heat and mass transfer in a Forchheimer porous medium.

The effect of solutal and thermal dispersion effects in homogeneous and isotropic Darcian porous media has been analyzed by Dagan [22]. A systematic derivation of the governing equations with various types of approximations used in applications has been presented. Using scale analysis arguments, Telles and Tre-

[1]Present address: Department of Mathematics and Humanities, REC Warangal, A.P., 506 004, India. E-mail: pvsnm@recw.ernet.in

Contributed by the Heat Transfer Division for publication in the JOURNAL OF HEAT TRANSFER. Manuscript received by the Heat Transfer Division, April 20, 1999; revision received, January 18, 2000. Associate Technical Editor: C. Beckermann.

visan [23] analyzed the double-dispersion phenomenon in a free-convection boundary layer adjacent to a vertical wall in a Darcian fluid-saturated porous medium. Depending on the relative magnitude of the dispersion coefficients, four classes of flow were identified and the heat and mass transfer has been studied.

In the present paper, the effect of hydrodynamic dispersion on mixed convection heat and mass transfer near a vertical surface embedded in a porous medium has been analyzed under boundary layer approximations using the similarity solution technique. The mixed convective flow is promoted by the uniform freestream and density variations due to the combination of temperature and concentration gradients. The Forchheimer flow model is considered and the porous medium porosity is assumed to be low so that the boundary effects in the medium may be neglected. The heat and mass transfer in the boundary layer region has been analyzed for aiding and opposing buoyancies for both the aiding and opposing flows. The flow, temperature, and concentration fields in Darcy and non-Darcy porous media are observed to be governed by complex interactions among the diffusion rate (Le), buoyancy ratio (N), and Pe_γ and Pe_ζ, the dispersion thermal and solutal diffusivity parameters, in addition to the flow driving parameter Ra/Pe. Due to dispersion effects, heat transfer is enhanced whereas the mass transfer coefficient becomes less predictable.

2 Governing Equations

Mixed convection heat and mass transfer from the impermeable vertical flat wall in a fluid-saturated porous medium is considered for the study and the schematic is shown in Fig. 1 (reproduced from Lai [4]). The x-axis is taken along the plate and y-axis is normal to it. The wall is maintained at constant temperature and concentration, T_w and C_w, respectively, and these values are assumed to be greater than the ambient temperature and concentration, T_∞ and C_∞, respectively. The governing equations for the boundary layer flow, heat, and mass transfer from the wall $y=0$ into the fluid-saturated porous medium $x \geqslant 0$ and $y>0$ (after making use of the Boussinesq approximation) are given by

$$\frac{\partial u}{\partial y}+\frac{c\sqrt{K}}{\nu}\frac{\partial u^2}{\partial y}=\left(\frac{Kg\beta_T}{\nu}\right)\frac{\partial T}{\partial y}+\left(\frac{Kg\beta_c}{\nu}\right)\frac{\partial C}{\partial y} \tag{1}$$

$$u\frac{\partial T}{\partial x}+v\frac{\partial T}{\partial y}=\frac{\partial}{\partial y}\left(\alpha_e\frac{\partial T}{\partial y}\right) \tag{2}$$

$$u\frac{\partial C}{\partial x}+v\frac{\partial C}{\partial y}=\frac{\partial}{\partial y}\left(D_e\frac{\partial C}{\partial y}\right) \tag{3}$$

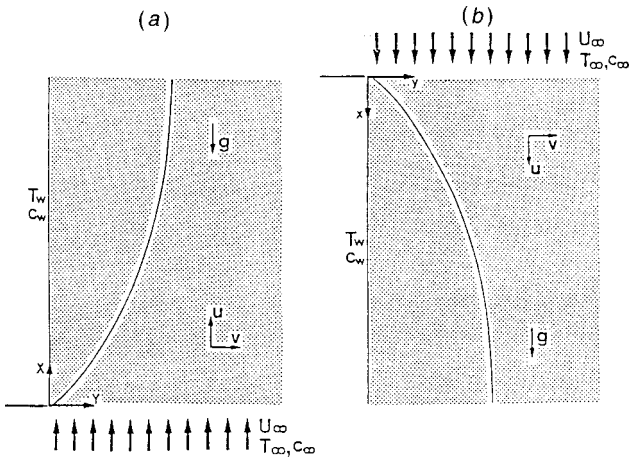

Fig. 1 Coupled heat and mass transfer by mixed convection from a vertical plate in a saturated porous medium (reproduced from Lai [4])

with the boundary conditions

$$\left.\begin{aligned} y=0: &\quad v=0, \quad T=T_w, \quad C=C_w \\ y\to\infty: &\quad u=u_\infty, \quad T=T_\infty, \quad C=C_\infty \end{aligned}\right\}. \tag{4}$$

Here x and y are the Cartesian coordinates, u and v are the averaged velocity components in x and y-directions, respectively, T is the temperature, C is the concentration, β_T is the coefficient of thermal expansion, β_C is the coefficient of solutal expansion, ν is the kinematic viscosity of the fluid, K is the permeability, c is an empirical constant, g is the acceleration due to gravity, and α_e and D_e are the effective thermal and solutal diffusivities, respectively. The subscripts w and ∞ indicate the conditions at the wall and at the outer edge of the boundary layer, respectively.

Following Telles and Trevisan [23], the expressions for α_e and D_e can be written as $\alpha_e=\alpha+\gamma du$ and $D_e=D+\zeta du$, where α and D are the molecular thermal and solutal diffusivities, respectively, whereas γdu and ζdu represent dispersion thermal and solutal diffusivities, respectively. The above model for thermal dispersion has been used extensively by researchers like Plumb [11], Hong et al. [13], Hong and Tien [12], Lai and Kulacki [2,15], Murthy and Singh [18,19,24] in studies of convective heat transfer in non-Darcy porous media. For moderate and high Peclet number flows, a linear variation of the thermal and solutal dispersions with velocity has been proved to be reasonable, see, for example, Saffman [25] and Bear [9]. Similar representation for solutal dispersion can be seen in Dagan [22].

Making use of the following transformation

$$\eta=\frac{y}{x}\mathrm{Pe}_x^{1/2}, \quad f(\eta)=\frac{\psi}{\alpha\mathrm{Pe}_x^{1/2}}, \quad \theta(\eta)=\frac{T-T_\infty}{T_w-T_\infty},$$

$$\phi(\eta)=\frac{C-C_\infty}{C_w-C_\infty},$$

the governing Eqs. (1)–(3) become

$$f''+2F_o\mathrm{Pe}f'f''=\pm\frac{\mathrm{Ra}}{\mathrm{Pe}}[\theta'+N\phi'] \tag{5}$$

$$\theta''+\frac{1}{2}f\theta'+\mathrm{Pe}_\gamma(f'\theta''+f''\theta')=0 \tag{6}$$

$$\phi''+\frac{\mathrm{Le}}{2}f\phi'+\mathrm{LePe}_\zeta(f'\phi''+f''\phi')=0 \tag{7}$$

and the boundary conditions (4) transform into

$$\left.\begin{aligned} \eta=0: &\quad f=0, \quad \theta=1, \quad \phi=1 \\ \eta\to\infty: &\quad f'=1, \quad \theta=0, \quad \phi=0 \end{aligned}\right\}. \tag{8}$$

The important parameters involved in the present study are the local Peclet number $\mathrm{Pe}_x=U_\infty x/\alpha$, the local Darcy-Rayleigh number $\mathrm{Ra}_x=Kg\beta_T\theta_w x/\alpha\nu$, which is defined with reference to the temperature difference alone, $\mathrm{Pe}=U_\infty d/\alpha$ and $\mathrm{Ra}=Kg\beta_T\theta_w d/\alpha\nu$, are the pore diameter-dependent Peclet and Rayleigh numbers, respectively. The inertial parameter is $F_o\mathrm{Pe}=(c\sqrt{K}\alpha/d\nu)(U_\infty d/\alpha)=c\sqrt{K}U_\infty/\nu$ (in the present study, $F_o\mathrm{Pe}$ is varied as a single parameter), the buoyancy ratio is $N=\beta_C\phi_w/\beta_T\theta_w$, and the diffusivity ratio is $\mathrm{Le}=\alpha/D$. The Lewis number is nothing but the ratio of the Schmidt number (ν/D) and Prandtl number (ν/α). The flow governing parameter is Ra/Pe and is independent of x. Ra/Pe=0 represents the forced convection flow. The flow asymptotically reaches the free convection flow limit as this parameter tends to ∞. Pe_γ and Pe_ζ represent thermal and solutal dispersion parameters, respectively, and are defined here as $\mathrm{Pe}_\gamma=\gamma U_\infty d/\alpha$ and $\mathrm{Pe}_\zeta=\zeta U_\infty d/\alpha$. It is worth mentioning that the thermal dispersion parameter Pe_γ has been treated as $\gamma\mathrm{Pe}$ in the works of Lai and Kulacki [26] where the coefficients of thermal dispersion have been assigned values in the range 1/7 to 1/3. Researchers like Gorla et al. [17], Hong and Tien [12], and

Hong et al. [13], who worked extensively on thermal dispersion effects, treated them as a single parameter ($Ds=\gamma$Ra), as the value of γ depends on the experiment. In the present investigation also, we consider the thermal and solutal dispersion parameters Pe_γ and Pe_ζ with γ and ζ included in the parameters. In Eq. (5), the positive and negative signs represent aiding and opposing flows, respectively. $N>0$ indicates the aiding buoyancy and $N<0$ indicates the opposing buoyancy.

3 Results and Discussion

The resulting ordinary differential Eqs. (5)–(7) are integrated by giving appropriate initial guess values for $f'(0)$, $\theta'(0)$, and $\phi'(0)$ to match the values with the corresponding boundary conditions at $f'(\infty)$, $\theta(\infty)$, and $\phi(\infty)$, respectively. NAG software (D02HAFE routine) is used for integrating the corresponding first-order system of equations and shooting and matching the initial and boundary conditions. The results are observed up to an accuracy of 5.0×10^{-6}. Extensive calculations have been performed to obtain the flow, temperature, and concentration fields for a wide range of parameters $0\leqslant F_o\mathrm{Pe}\leqslant 2$, $0\leqslant \mathrm{Ra/Pe}\leqslant 100$, $-1<N\leqslant 4$, $0.01\leqslant \mathrm{Le}\leqslant 100$, $0\leqslant \mathrm{Pe}_\gamma\leqslant 5$, and $0\leqslant \mathrm{Pe}_\zeta\leqslant 5$. As an indication of proper formulation and accurate calculation, the results obtained here are compared with previously published analytical results.

With $F_o\mathrm{Pe}=0$, $\mathrm{Pe}_\gamma=0$, and $\mathrm{Pe}_\zeta=0$, the present problem reduces to heat and mass transfer by Darcian mixed convection in porous media analyzed by Lai [4]. By setting the parameters $N=0$, $\mathrm{Le}=1$, and $\mathrm{Pe}_\zeta=0$, the problem reduces to that of non-Darcian mixed convection along a vertical wall in a saturated porous medium, which has been studied by Lai and Kulacki [15]. The comparison showed that the present results match exactly with the results presented in the above works. When N is comparable with -1, the temperature and concentration buoyancy effects are of the same order of magnitude and in opposing directions. Due to this, the resulting flow does not have the parallel double boundary layer structure. Contrary to what has been reported by Bejan and Khair [1], Lai and Kulacki [2] and Murthy and Singh [3] found similarity solutions for $\mathrm{Le}=1$ and $-1<N<0$, and the solutions in the range of $N<-1$ are impossible. These contradictions are resolved clearly in Lai and Kulacki [2]. In fact, the results presented below uncover some interesting facts regarding the flow field in the boundary layer, heat, and mass transfer coefficients.

3.1 Aiding Flow. When buoyancy is aiding the flow, for $N>0$ (aiding buoyancy case) the tangential velocity evolves from nonzero wall velocity to uniform freestream velocity for all values of $\mathrm{Le}>0$. In the case of opposing buoyancy ($N<0$), when $\mathrm{Le}>1$, the flow field follows the same pattern. But when $0<\mathrm{Le}<1$, a distinct feature is observed. The vertical component of velocity attains negative values near the wall and well inside the boundary layer. Far from the wall it attains its outer edge boundary condition. This may be explained as follows. When $N<0$ the downward species buoyancy overpowers the upward thermal buoyancy and $\mathrm{Le}<1$ results in larger solutal diffusion than the thermal diffusion. The favorable action of Ra/Pe to the flow field is countered by the opposing buoyancy ($N<0$) and also by the higher solutal diffusivity ($\mathrm{Le}<1$). The flow reversal is seen when the later effects dominate the flow favoring mixed convection parameter. This phenomena is clearly seen in Figs. 2 and 3. In these figures the tangential velocity component is plotted against similarity variable for $-1<N<0$ and $0<\mathrm{Le}<1$.

The Ra/Pe values indicated in the figures correspond to the minimum Ra/Pe for which flow reversal occurred under the fixed values of other parameters. For fixed Le, this value of Ra/Pe increases with the decrease in the value of the buoyancy ratio. For fixed value of buoyancy ratio N, this value of Ra/Pe increases with the increase in the value of the diffusion ratio Le. This phenomena is seen in both Darcy and non-Darcy mixed convection flows. It is also clear from both these figures that the inertial effects delay the occurrence of this phenomena. The work by Lai [4] did not reveal this phenomenon; recently Angirasa et al. [5] noticed flow reversal for $N=-0.5$ and -1.5 when $\mathrm{Le}<1$ in their study of free-convection heat and mass transfer in a fluid-saturated porous enclosure. They observed this phenomenon at large values of the flow-governing Rayleigh number. Mahajan and Angirasa [27] reported similar observations in connection with free-convection heat and mass transfer in the case of opposing buoyancies in clear fluids also.

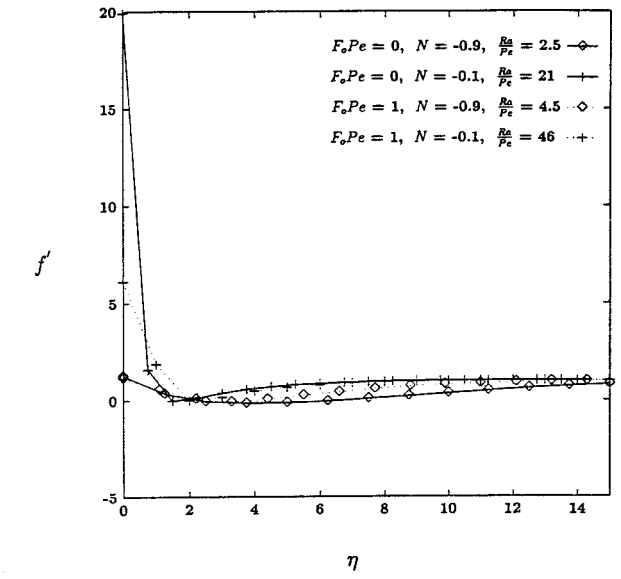

Fig. 2 Nondimensional velocity profiles $f'(\eta)$ for $-1<N<0$, $\mathrm{Le}=0.1$ (aiding flow)

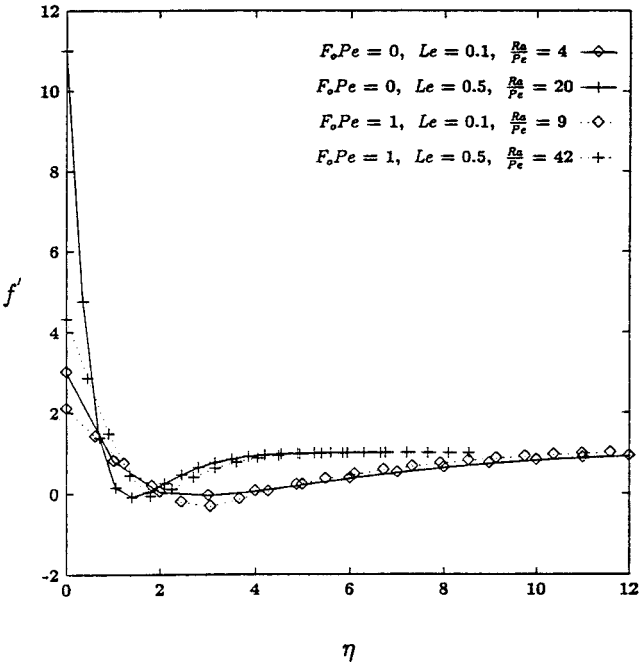

Fig. 3 Nondimensional velocity profiles $f'(\eta)$ for $0<\mathrm{Le}<1$, $N=-0.5$ (aiding flow)

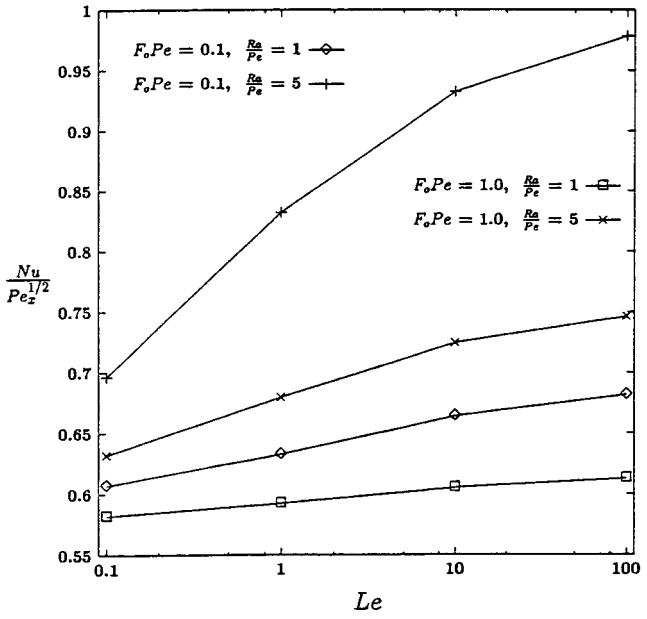

Fig. 4 Heat transfer coefficient as a function of Lewis number when $N<0$. Here $N=-0.5$, $Pe_\gamma=0=Pe_\zeta$ (aiding flow).

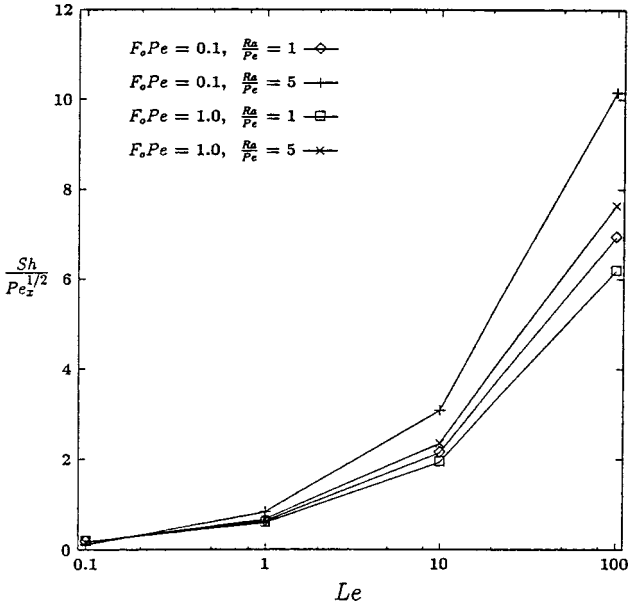

Fig. 6 Mass transfer coefficient as a function of Lewis number when $N<0$. Here $N=-0.5$, $Pe_\gamma=0=Pe_\zeta$ (aiding flow).

Now the heat and mass transfer coefficients, in terms of the Nusselt and Sherwood numbers in the presence of thermal and solutal dispersion diffusivities, can be written as

$$\frac{\mathrm{Nu}}{\mathrm{Pe}_x^{1/2}} = -[1+\mathrm{Pe}_\gamma f'(0)]\theta'(0), \tag{9}$$

$$\frac{\mathrm{Sh}}{\mathrm{Pe}_x^{1/2}} = -[1+\mathrm{Pe}_\zeta f'(0)]\phi'(0). \tag{10}$$

With $F_o\mathrm{Pe}=0$, $\mathrm{Pe}_\gamma=0$, and $\mathrm{Pe}_\zeta=0$, the observations made here are consistent with those reported by Lai [4]. It is observed that for $\mathrm{Le}>1$, the heat transfer coefficient increases for $N<0$ and it decreases for $N>0$. For $\mathrm{Le}<1$, the situation is reversed. For $\mathrm{Pe}_\gamma=0$ and $\mathrm{Pe}_\zeta=0$, the Eqs. (9) and (10) reduce to $\mathrm{Nu}/\mathrm{Pe}_x^{1/2}=-\theta'(0)$ and $\mathrm{Sh}/\mathrm{Pe}_x^{1/2}=-\phi'(0)$. The effect of diffusivity ratio and the buoyancy ratio on heat and mass transfer coefficients is plotted in Figs. 4–7 for two values of inertial parameter $F_o\mathrm{Pe}=0.1$ (near Darcy-region) and $F_o\mathrm{Pe}=1.0$ (non-Darcy region). The inertial effects always decrease the heat and mass transfer coefficients in both opposing and aiding buoyancies. The increase in the value of the mixed convection parameter increases the heat and mass transfer rates. It is clearly seen from these figures that the convection favoring effect of Ra/Pe is countered by the microscopic drag due to the increase in the inertial parameter. The heat transfer coefficient is observed to increase with the diffusivity ratio in the opposing buoyancy case whereas it decreases in the aiding buoyancy case. This is clearly seen from

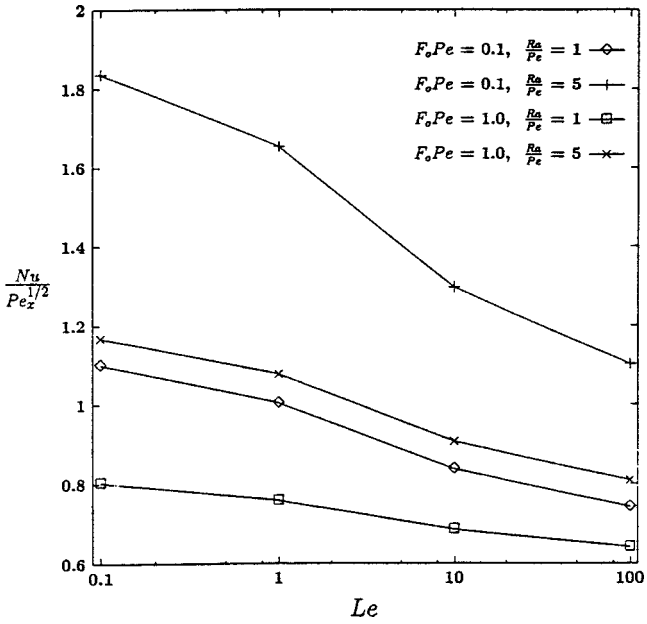

Fig. 5 Heat transfer coefficient as a function of Lewis number when $N>0$. Here, $N=4.0$, $Pe_\gamma=0=Pe_\zeta$ (aiding flow).

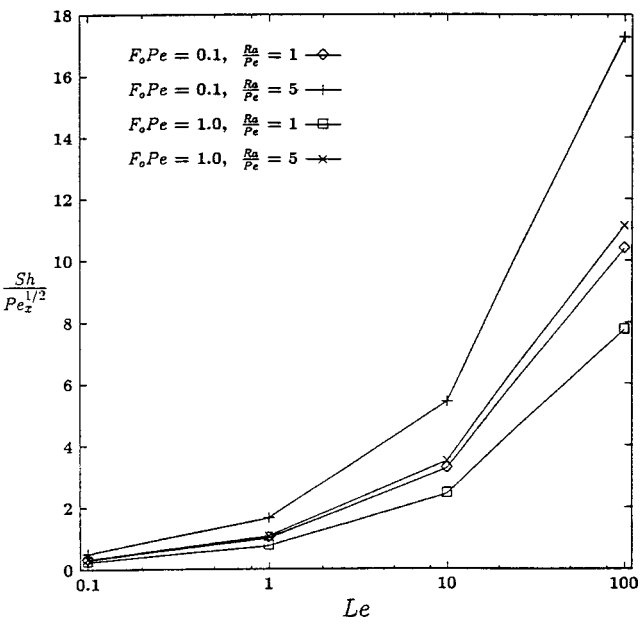

Fig. 7 Mass transfer coefficient as a function of Lewis number when $N>0$. Here, $N=4.0$, $Pe_\gamma=0=Pe_\zeta$ (aiding flow).

Table 1 $-\theta'(0)$ **for** $N=-0.5$, $F_o\mathrm{Pe}=1.0$ **and** $\mathrm{Pe}_\zeta=0$

		Le=1			Le=10		
Ra/Pe	$f'(0)$	$\mathrm{Pe}_\gamma=0$	$\mathrm{Pe}_\gamma=1$	$\mathrm{Pe}_\gamma=5$	$\mathrm{Pe}_\gamma=0$	$\mathrm{Pe}_\gamma=1$	$\mathrm{Pe}_\gamma=5$
0	1.0	0.5642	0.3989	0.2303	0.5642	0.3989	0.2303
1	1.1583	0.5922	0.4027	0.2305	0.6054	0.4151	0.2368
5	1.6794	0.6793	0.4186	0.2354	0.7244	0.4544	0.2500
10	2.1926	0.7580	0.4344	0.2405	0.8247	0.4801	0.2568
20	3.0	0.8706	0.4557	0.2465	0.9617	0.5069	0.2627
50	4.7262	1.0768	0.4870	0.2541	1.203	0.5387	0.2684
100	6.7284	1.2797	0.5096	0.2588	1.4347	0.5581	0.2713

Table 2 $-\theta'(0)$ **for** $N=1.0$, $F_o\mathrm{Pe}=1.0$ **and** $\mathrm{Pe}_\zeta=0$

		Le=1			Le=10		
Ra/Pe	$f'(0)$	$\mathrm{Pe}_\gamma=0$	$\mathrm{Pe}_\gamma=1$	$\mathrm{Pe}_\gamma=5$	$\mathrm{Pe}_\gamma=0$	$\mathrm{Pe}_\gamma=1$	$\mathrm{Pe}_\gamma=5$
0	1.0	0.5642	0.3989	0.2303	0.5642	0.3989	0.2303
1	1.5616	0.6603	0.3892	0.1984	0.6377	0.3706	0.1901
5	3.0	0.8706	0.3771	0.1695	0.8083	0.3411	0.1576
10	4.217	1.0203	0.3714	0.1609	0.9358	0.3323	0.1494
20	6.0	1.2097	0.3657	0.1552	1.1012	0.3269	0.1449
50	9.6119	1.5295	0.3585	0.1507	1.3837	0.3234	0.1423
100	13.7215	1.8237	0.3535	0.1488	1.6492	0.3221	0.1415

Figs. 4 and 5. For fixed values of other parameters, the magnitude of $\mathrm{Nu}/\mathrm{Pe}_x^{1/2}$ for $N>0$ is higher than that for $N<0$ for all values of Le considered in the study. This clearly indicates that the buoyancy ratio has significant effect on the heat transfer coefficient than the diffusivity ratio. Figures 6 and 7 clearly indicate the favorable effect of the Lewis number on the mass transfer coefficient in both opposing and aiding buoyancies. Uniform trend in the Sherwood number results is observed with increase in the buoyancy ratio N from -1 to 4.

The variation of the heat transfer coefficient with Ra/Pe for nonzero values of Pe_γ is studied for a wide range of values of Le. The effect of thermal dispersion on the heat transfer is studied keeping $\mathrm{Pe}_\zeta=0$. Consistent with the results presented in Lai and Kulacki [15] and Hong and Tien [12], the value of $-\theta'(0)$ decreases as the thermal dispersion coefficient Pe_γ increases. Also

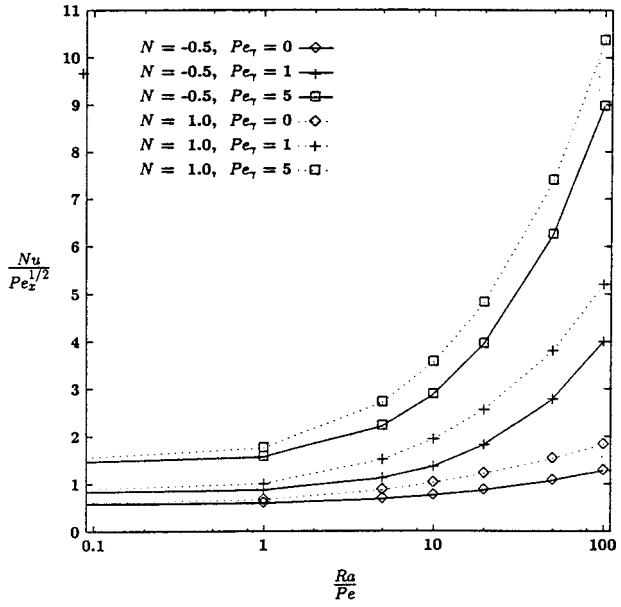

Fig. 8 Heat transfer coefficient as a function of Ra/Pe when $F_o\mathrm{Pe}=1.0$, $\mathrm{Le}=1.0$, $\mathrm{Pe}_\zeta=0$ **(aiding flow)**

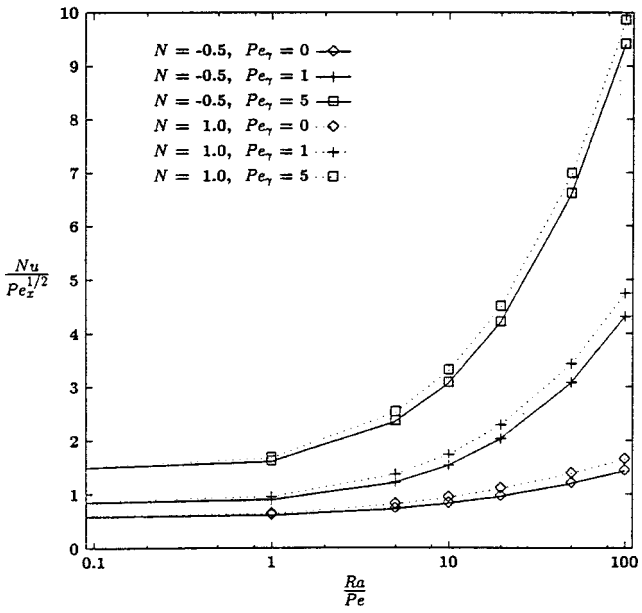

Fig. 9 Heat transfer coefficient as a function of Ra/Pe when $F_o\mathrm{Pe}=1.0$, $\mathrm{Le}=10.0$, $\mathrm{Pe}_\zeta=0$ **(aiding flow)**

for large Pe_γ, in a very small region near the wall, the temperature gradient is greatly increased and as a result heat transfer is greatly enhanced due to thermal dispersion. The wall temperature gradient values for $F_o\mathrm{Pe}=1$, for two values of $N=-0.5$ and 1.0 are presented in Tables 1–2. The value of $f'(0)$ is dependent on $F_o\mathrm{Pe}$ and this is evident from the previous studies as well. From these two tables, it is also clear that $f'(0)$ depends on the buoyancy ratio N. The heat transfer coefficient written in terms of the Nusselt number using Eq. (9) is calculated from the values of $-\theta'(0)$ for the nonzero dispersion coefficient and is plotted in Figs. 8–9 for Le=1.0 and 10.0, respectively. Figures clearly indicate the favorable influence of thermal dispersion on the heat transfer results. The $\mathrm{Nu}/\mathrm{Pe}_x^{1/2}$ value increases with increasing Ra/Pe. Aiding buoyancy favors the heat transfer, whereas this favorable action is aided by increasing the value of Le when $N<0$ and is suppressed by an increase in the value of Le when $N>0$. This is evident from the Figs. 8–9. These results are in agreement with the results reported by Lai [4].

The effect of solutal dispersion on the mass transfer coefficient has been analyzed keeping $\mathrm{Pe}_\gamma=0$. The values of $-\phi'(0)$ have been tabulated for $F_o\mathrm{Pe}=1$ and for two values of $N=-0.5$ and 1.0 in Tables 3–4. Analogous to the pure thermal convection process, the value of $-\phi'(0)$ decreases with increasing values of Pe_ζ. Interestingly, at large Pe_ζ, for large values of Ra/Pe, in a relatively large region (larger than that observed for thermal gradients) near the wall, the concentration gradient is greatly increased. But, against this expectation, peculiar behavior in the mass transfer coefficient is observed. The imbalance between the

Table 3 $-\phi'(0)$ **for** $N=-0.5$, $F_o\mathrm{Pe}=1.0$ **and** $\mathrm{Pe}_\gamma=0$

		Le=1			Le=10		
Ra/Pe	$f'(0)$	$\mathrm{Pe}_\gamma=0$	$\mathrm{Pe}_\gamma=1$	$\mathrm{Pe}_\gamma=5$	$\mathrm{Pe}_\gamma=0$	$\mathrm{Pe}_\gamma=1$	$\mathrm{Pe}_\gamma=5$
0	1.0	0.5642	0.3989	0.2303	1.7841	0.5379	0.2498
1	1.1583	0.5922	0.3888	0.2062	1.9329	0.512	0.2208
5	1.6794	0.6793	0.3555	0.1463	2.3534	0.4463	0.1534
10	2.1926	0.758	0.3258	0.105	2.7009	0.3992	0.1109
20	3.0	0.8706	0.2835	0.0716	3.1686	0.3441	0.0769
50	4.7262	1.0768	0.219	0.0483	3.9815	0.2678	0.0515
100	6.7284	1.2797	0.1801	0.0383	4.7585	0.2168	0.0403

Table 4 $-\phi'(0)$ for $N=1.0$, $F_o\mathrm{Pe}=1.0$ and $\mathrm{Pe}_\gamma=0$

		Le=1			Le=10		
Ra/Pe	$f'(0)$	$\mathrm{Pe}_\gamma=0$	$\mathrm{Pe}_\gamma=1$	$\mathrm{Pe}_\gamma=5$	$\mathrm{Pe}_\gamma=0$	$\mathrm{Pe}_\gamma=1$	$\mathrm{Pe}_\gamma=5$
0	1.0	0.5642	0.3989	0.2303	1.7841	0.5379	0.2498
1	1.5616	0.6603	0.3892	0.1984	2.1381	0.4773	0.2078
5	3.0	0.8706	0.3771	0.1695	2.8864	0.4215	0.1728
10	4.217	1.0203	0.3714	0.1609	3.4061	0.4018	0.1629
20	6.0	1.2097	0.3657	0.1552	4.0548	0.3858	0.1564
50	9.6119	1.5295	0.3585	0.1507	5.1295	0.3698	0.1514
100	13.7215	1.8237	0.3535	0.1488	6.1278	0.3607	0.1492

Lewis number and buoyancy parameter influence more against the enhancement of mass transfer results. For $\mathrm{Pe}_\zeta=0$, the value of $-\phi'(0)$ increases with increasing values of Ra/Pe for all values of Le and N. For large Pe_ζ, the value of $-\phi'(0)$ decreases rapidly to near zero values with increasing Ra/Pe.

The mass transfer results are not straightforward for analysis. The complex interaction between Le, N, Pe_ζ, and Ra/Pe show complex behavior for $\mathrm{Sh}/\mathrm{Pe}_x^{1/2}$ curves. The results presented in the Figs. 10 and 11 are for Le=1 and 10 with $F_o\mathrm{Pe}=1$ and $\mathrm{Pe}_\gamma=0$. In the case of aiding buoyancy, when Le=1, the mass transfer coefficient increases with Ra/Pe and the dispersion mechanism augments the mass transfer. In fact, these curves are same as the curves presented for $N=1.0$ in Fig. 8 (see the Eqs. (5)–(7) with Le=1). But this is not the case in the opposing buoyancy. When $N<0$ and Le=1, $\mathrm{Sh}/\mathrm{Pe}_x^{1/2}$ increases with Ra/Pe for $\mathrm{Pe}_\zeta=0$ and $\mathrm{Pe}_\zeta=1$. When $\mathrm{Pe}_\zeta=5$, it increases with Ra/Pe up to the value 5 and then decreases thereafter. Its value becomes less than the corresponding value for $\mathrm{Pe}_\zeta=1$ from Ra/Pe=20 onwards; it may be inferred that the strength of the solutal dispersion becomes insignificant at higher values of Ra/Pe in the case of opposing buoyancy.

Unlike when Le=1, for Le>1, even for $N>0$, there is no clear pattern for the mass transfer results. From Fig. 11 it can be observed that the curve for $\mathrm{Pe}_\zeta=1$ is always at a lower level than that for $\mathrm{Pe}_\zeta=0$. Also, the curve for $\mathrm{Pe}_\zeta=5$ is at a lower level up to Ra/Pe=5 and from that point onwards the $\mathrm{Sh}/\mathrm{Pe}_x^{1/2}$ values are greater than the corresponding values of that for $\mathrm{Pe}_\zeta=0$. This shows clearly that in the aiding buoyancy case, for moderate to large values of Le, the effect of the dispersion parameter is not favorable for the mass transfer up to a certain low value of Ra/Pe. Also, there exists a critical value of Ra/Pe after which the dispersion effects are significant in the mass transfer mechanism. With Le=10 and $N<0$, the $\mathrm{Sh}/\mathrm{Pe}_x^{1/2}$ curve for $\mathrm{Pe}_\zeta=0$ is always at a higher level than that for $\mathrm{Pe}_\zeta=1$ and 5. This shows that as the value of the Lewis number increases, the dispersion effects reduce the mass transfer rate at moderate and higher values of Ra/Pe in the opposing buoyancy. Thus the complex interactions between $F_o\mathrm{Pe}$, Le, N, Ra/Pe and the pair Pe_γ and Pe_ζ prevent us from making any general statement about the mass transfer mechanism.

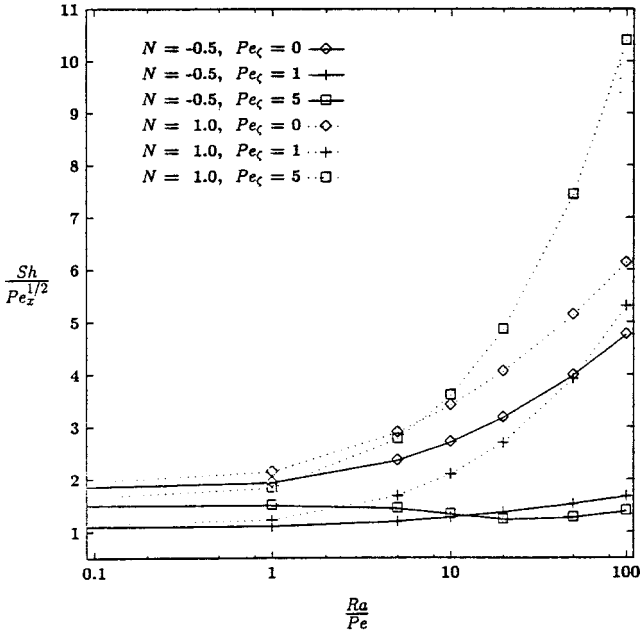

Fig. 11 Mass transfer coefficient as a function of Ra/Pe when $F_o\mathrm{Pe}=1.0$, Le=10.0, $\mathrm{Pe}_\gamma=0$ (aiding flow)

3.2 Opposing Flow. The flow field becomes more complex when the freestream flow is opposing the buoyancy. Like in the

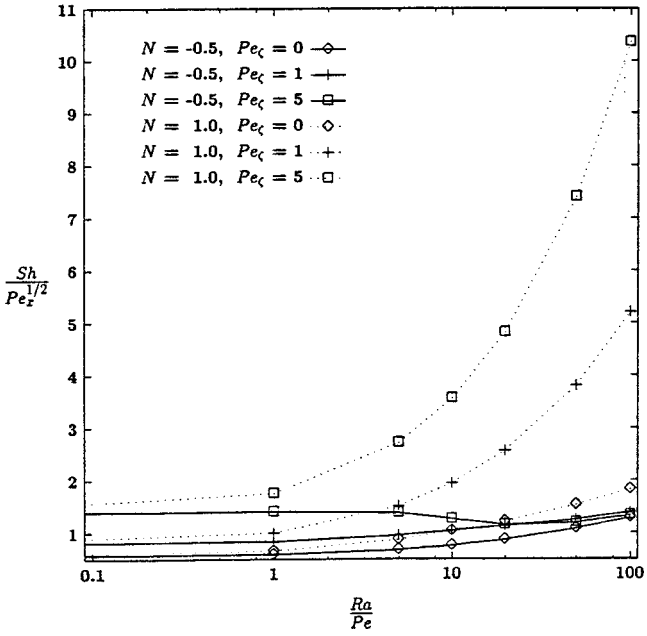

Fig. 10 Mass transfer coefficient as a function of Ra/Pe when $F_o\mathrm{Pe}=1.0$, Le=1.0, $\mathrm{Pe}_\gamma=0$ (aiding flow)

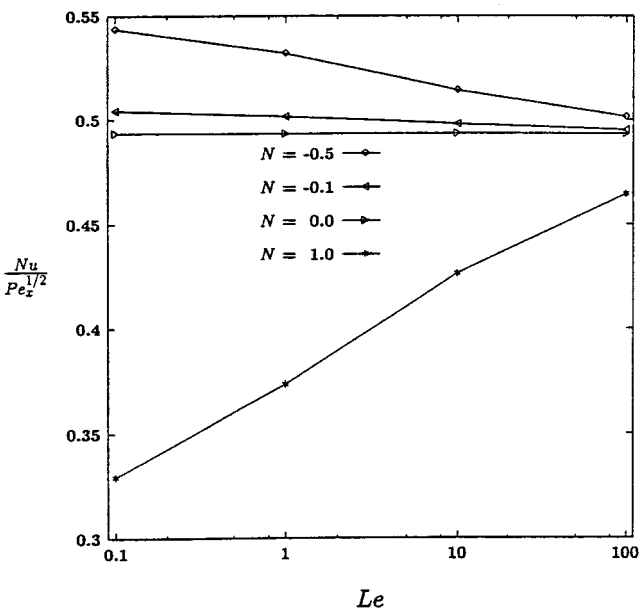

Fig. 12 Heat transfer coefficient as a function of Le for various values of N when $\mathrm{Pe}_\gamma=0=\mathrm{Pe}_\zeta$, Ra/Pe=1.0, $F_o\mathrm{Pe}=1.0$ (opposing flow)

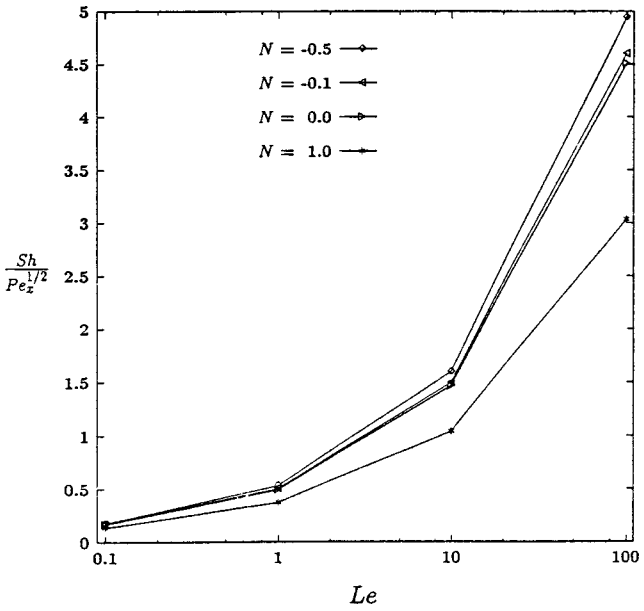

Fig. 13 Mass transfer coefficient as a function of Le for various values of N when $Pe_\gamma = 0 = Pe_\zeta$, Ra/Pe=1.0, F_oPe=1.0 (opposing flow)

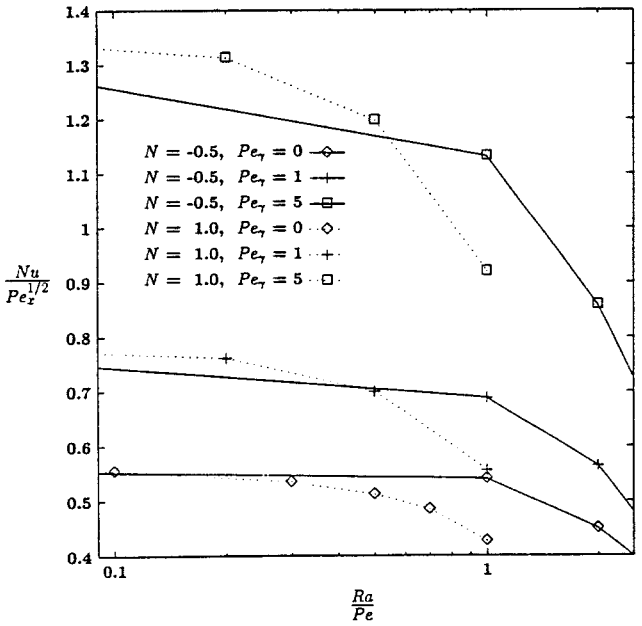

Fig. 15 Heat transfer coefficient as a function of Ra/Pe in the presence of thermal dispersion effects in non-Darcy flow. Here F_oPe=1.0, Le=10.0, $Pe_\zeta = 0$ (opposing flow).

aiding flow case, the wall velocity depends only on the inertial parameter and the buoyancy ratio. It is independent on the Lewis number. Flow separation is the most common feature observed in the opposing flows. The flow separation point also depends on the buoyancy ratio. In the absence of thermal and solutal dispersion effects, the separation point in the Darcy flow (F_oPe=0) is seen to occur at Ra/Pe=2.0, 1.1, 1, 0.5 for $N=-0.5$, -0.1, 0, 1.0, respectively. In the Forchheimer flow (F_oPe=1.0) the occurence of the flow separation is delayed, the separation points are observed to occur at Ra/Pe=4.0, 2.3, 2.0, 1.0 for $N=-0.5$, -0.1, 0, 1.0, respectively. The presence of thermal and solutal dispersion diffusivity will not alter the point of flow separation in both Darcy and non-Darcy flows.

The heat and mass transfer coefficients in opposing flow are presented in Figs. 12–17. As expected, the heat transfer decreases with Le for opposing buoyancy, whereas it increases with Le for aiding buoyancy. It is just a reverse mechanism to the aiding flow case and is clearly seen in Fig. 12. The $Nu/Pe_x^{1/2}$ values for the opposing buoyancy are at higher level than those for aiding buoyancy. It is evident from the Fig. 13 that the mass transfer coefficient increases with Le here also, the $Sh/Pe_x^{1/2}$ values in opposing buoyancy are at higher level than those in aiding buoyancy. Aid-

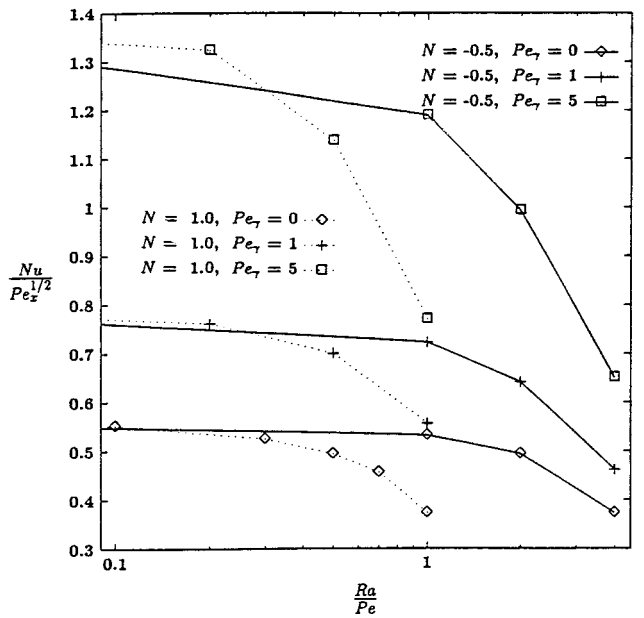

Fig. 14 Heat transfer coefficient as a function of Ra/Pe in the presence of thermal dispersion effects in non-Darcy flow. Here F_oPe=1.0, Le=1.0, $Pe_\zeta = 0$ (opposing flow).

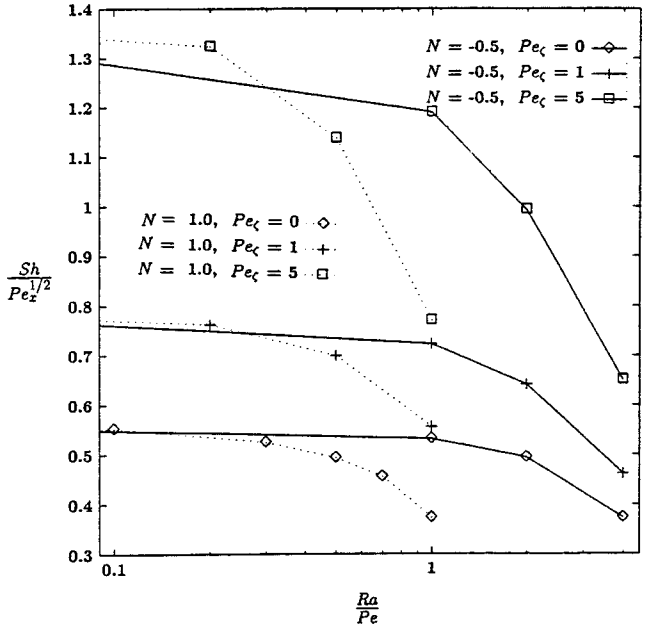

Fig. 16 Mass transfer coefficient as a function of Ra/Pe in the presence of solutal dispersion effects in non-Darcy flow. Here F_oPe=1.0, Le=1.0, $Pe_\gamma = 0$ (opposing flow).

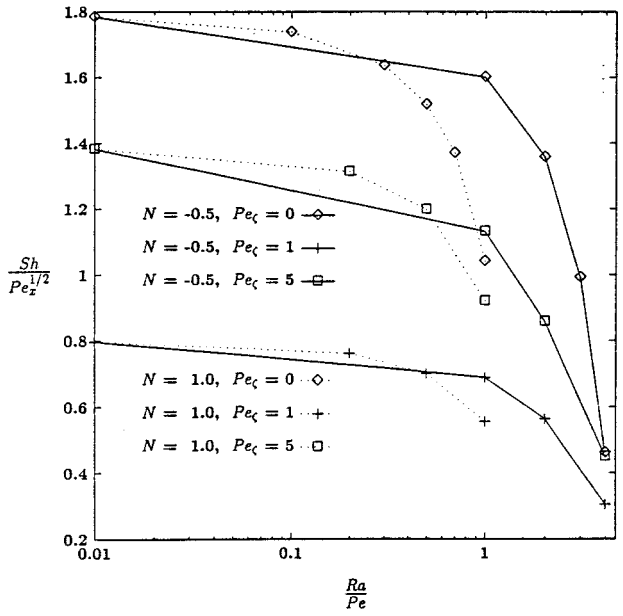

Fig. 17 Mass transfer coefficient as a function of Ra/Pe in the presence of solutal dispersion effects in non-Darcy flow. Here F_oPe=1.0, Le=10.0, Pe$_\gamma$=0 (opposing flow).

ing buoyancy is hindrance to the free stream flow in the opposing flow case, so a reduction in the transport quantities is observed.

The variation of $\mathrm{Nu/Pe}_x^{1/2}$ with Ra/Pe in the opposing flow is plotted in Figs. 14–15 with $F_o\mathrm{Pe}=1$ for different values of N and Pe_γ. Thermal dispersion enhances the heat transfer rate in both $N>0$ and $N<0$ for all values of Le>0. Interestingly, for fixed Le, and nonzero Pe_γ, there exists one critical value of Ra/Pe before which the $\mathrm{Nu/Pe}_x^{1/2}$ for $N=1.0$ is more than that for $N=-0.5$ and after which its reverse is seen. These arguments are evident from Figs. 14–15.

The $\mathrm{Sh/Pe}_x^{1/2}$ is plotted against Ra/Pe for $F_o\mathrm{Pe}=1$ and for six combinations of Pe_ζ and N in Figs. 16–17. Here also, the mass transfer coefficient decreases with Ra/Pe, the dispersion effect enhances the mass transfer, and the existence of critical Ra/Pe for which the dual behavior of the mass transfer coefficient is observed. In the opposing flow also, the complex interactions between these parameters do not permit a clear pattern for the heat and mass transfer results.

Conclusions

Similarity solution for hydrodynamic dispersion in mixed convection heat and mass transfer near vertical surface embedded in a porous medium has been presented. The heat and mass transfer in the boundary layer region has been analyzed for aiding and opposing buoyancies in both the aiding and opposing flows. The structure of the flow, temperature, and concentration fields in the Darcy and non-Darcy porous media are governed by complex interactions among the diffusion rates (Le) and buoyancy ratio (N) in addition to the flow driving parameter (Ra/Pe). Extensive calculations for a wide range of these parameters are performed. For small values of Le in the opposing buoyancy, flow reversal near the wall is observed. The heat transfer coefficient always increases with Ra/Pe. Thermal dispersion favors the heat transfer. As Le increases, the effect of solutal dispersion on the nondimensional mass transfer coefficient becomes less predictable in both aiding and opposing buoyancies. In the opposing flow case, the flow separation point is observed to depend on the inertial parameter and buoyancy ratio. A reduction in the heat and mass transfer coefficients is seen with increasing values of Ra/Pe. Here also the Lewis number has complex impact on the heat and mass transfer mechanism.

Acknowledgments

My sincere thanks to the reviewers for their encouraging comments and constructive suggestions to improve the manuscript. I thank Prof. A. Avudainayagam, Department of Mathematics, IIT–Madras for his constant encouragement and support during my post-doctoral research. I sincerely acknowledge the CSIR (INDIA) for its financial support in carrying out this research.

Nomenclature

c = inertial coefficient
C = concentration
d = pore diameter
D = mass diffusivity
D_e = effective mass diffusivity
f = nondimensional stream function
$F_o\mathrm{Pe}$ = $c\sqrt{K}U_\infty/\nu$, parameter representing non-Darcian effects
g = acceleration due to gravity
K = permeability
Le = α/D, Lewis number
N = $\beta_C\phi_w/\beta_T\theta_w$, buoyancy ratio
$\mathrm{Nu/Pe}_x^{1/2}$ = nondimensional heat transfer coefficient; ref Eq. (9)
$\mathrm{Sh/Pe}_x^{1/2}$ = nondimensional mass transfer coefficient; ref Eq. (10)
Pe_x = local Peclet number $u_\infty x/\alpha$
Pe = $u_\infty d/\alpha$
Pe_γ = $\gamma U_\infty d/\alpha$, parameter representing thermal dispersion effects
Pe_ζ = $\zeta U_\infty d/\alpha$, parameter representing solutal dispersion effects
Ra_x = modified Rayleigh number, $Kg\beta_T\theta_w x/\alpha\nu$
Ra = $Kg\beta_T\theta_w d/\alpha\nu$
T = temperature
u,v = velocity components in x and y-directions, respectively
x, y = Cartesian coordinates

Greek Symbols

α = molecular thermal diffusivity
α_e = effective thermal diffusivity
β_T = thermal expansion coefficient
β_C = solutal expansion coefficient
η = similarity variable
ν = kinematic viscosity
ψ = stream function
θ = nondimensional temperature
ϕ = nondimensional concentration
γ = coefficient of dispersion thermal diffusivity
ζ = coefficient of dispersion solutal diffusivity

Subscripts

w = evaluated at wall
∞ = evaluated at the outer edge of the boundary layer

References

[1] Bejan, A., and Khair, K. R., 1985, ''Heat and Mass Transfer by Natural Convection in a Porous Medium,'' Int. J. Heat Mass Transf., **28**, pp. 909–918.
[2] Lai, F. C., and Kulacki, F. A., 1991a, ''Coupled Heat and Mass Transfer by Natural Convection From Vertical Surfaces in Porous Media,'' Int. J. Heat Mass Transf., **34**, pp. 1189–1194.
[3] Murthy, P. V. S. N., and Singh, P., 1998, ''Heat and Mass Transfer by Natural Convection in a Non-Darcy Porous Medium,'' Acta Mech., accepted for publication.
[4] Lai, F. C., 1991, ''Coupled Heat and Mass Transfer by Mixed Convection From a Vertical Plate in a Saturated Porous Medium,'' Int. Commun. Heat Mass Transfer, **18**, pp. 93–106.

[5] Angirasa, D., Peterson, G. P., and Pop, I., 1997, ''Combined Heat and Mass Transfer by Natural Convection With Opposing Buoyancy Effects in a Fluid Saturated Porous Medium,'' Int. J. Heat Mass Transf., **40**, pp. 2755–2773.
[6] Vafai, K., and Tien, C. L., 1981, ''Boundary and Inertia Effects on Flow and Heat Transfer in Porous Media,'' Int. J. Heat Mass Transf., **24**, pp. 195–203.
[7] Vafai, K., and Tien, C. L., 1982, ''Boundary and Inertia Effects on Convective Mass Transfer in Porous Media,'' Int. J. Heat Mass Transf., **25**, pp. 1183–1190.
[8] Whitaker, S., 1997, ''The Forchheimer Equation: A Theoretical Development,'' Transp. Porous Media, **25**, pp. 27–61.
[9] Bear, J., 1972, *Dynamics of Fluids in Porous Media*, Elsevier, New York.
[10] Kvernvold, O., and Tyvand, P., 1980, ''Dispersion Effect on Thermal Convection in Porous Media,'' J. Fluid Mech., **99**, pp. 673–686.
[11] Plumb, O. A., 1981, ''The Effect of Thermal Dispersion on Heat Transfer in Packed Bed Boundary Layers,'' *ASME-JSME Joint Thermal Conference Proceedings*, Vol. 2, ASME, New York, pp. 17–21.
[12] Hong, J. T., and Tien, C. L., 1987, ''Analysis of Thermal Dispersion Effect on Vertical Plate Natural Convection in Porous Media,'' Int. J. Heat Mass Transf., **30**, pp. 143–150.
[13] Hong, J. T., Yamada, Y., and Tien, C. L., 1987, ''Effect of Non-Darcian and Non-Uniform Porosity on Vertical Plate Natural Convection in Porous Media,'' ASME J. Heat Transfer, **109**, pp. 356–362.
[14] Cheng, P., and Vortmeyer, D., 1988, ''Transverse Thermal Dispersion and Wall Channeling in a Packed Bed With Forced Convection Flow,'' Chem. Eng. Sci., **43**, pp. 2523–2532.
[15] Lai, F. C., and Kulacki, F. A., 1991b, ''Non-Darcy Mixed Convection Along a Vertical Wall in Saturated Porous Medium,'' ASME J. Heat Transfer, **113**, pp. 252–255.
[16] Amiri, A., and Vafai, K., 1994, ''Analysis of Dispersion Effects and Non-Theormal Equilibrium, Non-Darcian, Variable Porosity Incompressible Flow Through Porous Media,'' Int. J. Heat Mass Transf., **37**, pp. 936–954.
[17] Gorla, R. S. R., Bakier, A. Y., and Byrd, L., 1996, ''Effects of Thermal Dispersion and Stratification on Combined Convection on a Vertical Surface Embedded in a Porous Medium,'' Transp. Porous Media, **25**, pp. 275–282.
[18] Murthy, P. V. S. N., and Singh, P., 1997, ''Effect of Viscous Dissipation on a Non-Darcy Natural Convection Regime,'' Int. J. Heat Mass Transf., **40**, pp. 1251–1260.
[19] Murthy, P. V. S. N., and Singh, P., 1997, ''Thermal Dispersion Effects on Non-Darcy Natural Convection Over Horizontal Plate With Surface Mass Flux,'' Arch. Appl. Mech., **67**, pp. 487–495.
[20] Nield, D. A., and Bejan, A., 1992, *Convection in Porous Media*, Springer-Verlag, New York.
[21] Karimi-Fard, M., Charrier-Mojtabi, M. C., and Vafai, K., 1997, ''Non-Darcian Effects on Double-Diffusive Convection Within a Porous Medium,'' Numer. Heat Transfer, Part A, **31**, pp. 837–852.
[22] Dagan, G., 1972, ''Some Aspects of Heat and Mass Transport in Porous Media,'' *Developments in Soil Science: Fundamentals of Transport Phenomena in Porous Media*, International Association for Hydraulic Research, Elsevier, London, pp. 55–63.
[23] Telles, R. S., and Trevisan, O. V., 1993, ''Dispersion in Heat and Mass Transfer Natural Convection Along Vertical Boundaries in Porous Media,'' Int. J. Heat Mass Transf., **36**, pp. 1357–1365.
[24] Murthy, P. V. S. N., and Singh, P., 1997, ''Thermal Dispersion Effects on Non-Darcy Natural Convection With Lateral Mass Flux,'' Heat Mass Transfer, **33**, pp. 1–5.
[25] Saffman, P. G., 1960, ''Dispersion due to Molecular Diffusion and Macroscopic Mixing in Flow Through a Network of Capillaries,'' J. Fluid Mech., **7**, pp. 194–208.
[26] Lai, F. C., and Kulacki, F. A., 1989, ''Thermal Dispersion Effects on Non-Darcy Convection Over Horizontal Surfaces in Saturated Porous Media,'' Int. J. Heat Mass Transf., **32**, pp. 356–362.
[27] Mahajan, R. L., and Angirasa, D., 1993, ''Combined Heat and Mass Transfer by Natural Convection With Opposing Buoyancies,'' ASME J. Heat Transfer, **115**, pp. 606–612.